

Extracellular biosynthesis of silver nanoparticles using entamopathogenic bacteria against *Meloidogyne incognita*

A. Vinothini, S. Iruthaya Kalai Selvam*

Vinothini A, Selvam SIK. Extracellular biosynthesis of silver nanoparticles using entamopathogenic bacteria against *Meloidogyne incognita*. *AGBIR*.2022;38(6):395-400.

Background: Root-knot nematode *Meloidogyne incognita* represents one of the most significant genera of plant-parasitic nematodes on various crops, as it is widespread and poses a threat to thousands of plant species. As a result of their infection of the root system, which absorbs water and nutrients, the entire plant is harmed. Their population expands at a quick rate as a result of the fact that at least two life cycles can be completed within the span of a particular growing season and that females have a high rate of fertility. The use of chemical nematicides to control the pathogen has been restricted due to adverse environmental and health effects. Now widely accepted as a substitute for agrochemicals, silver eliminates unwanted microorganisms in planter soils and hydroponics systems. Silver nanoparticles are also an excellent stimulant of plant growth. Silver nanoparticles have potent antibacterial, antifungal, insecticidal, and nematicidal properties.

Methods: The supernatant of symbiotic bacteria *Photobacterium luminescens* ON929969 from the entamopathogenic was employed for the synthesis of silver (PsAgNPs) nanoparticles. UV-visible spectrophotometer, X-ray diffraction analysis, Fourier transform infrared spectroscopy, and scanning electron microscopy studies were used to characterize the produced AgNPs. To examine the larvicidal impact of bio PsAgNPs, each treatment was

duplicated three times in CRD. Observations were made on the mortality of *M. incognita* juveniles every 24 hours, and the percentage mortality of juveniles was calculated after confirming the irreversible reaction of *M. incognita* upon exposure to the bio-synthesised PsAgNPs.

Results: UV-visible spectroscopic investigation has revealed that PsAgNPs have a prominent SPR peak at 430 nm. Synthesized AgNPs exhibited frequency bands at 3398.50, 2960.04, 1641.39, 1540.52, 1387.38, 1230.45, 1077.11, and 607.03 cm^{-1} , as confirmed by FTIR. The Debye-Scherrer equation reveals that the average crystallite size of produced AgNP is 22.38 nm. The results clearly demonstrate that the majority of AgNPs were aggregated spherical nanoparticles with a distinct size distribution and an average diameter of approximately 15.5 nm. The effect of bio PsAgNPs had a direct correlation between the death rate of J2 of *M. incognita* and exposure concentrations/duration. There was 100 percent death of *M. incognita* juveniles at higher concentrations of 2 and 3 g/ml of bio-synthesized AgNPs during the shortest duration of time of 24 hours, and this tendency was maintained throughout the exposure period.

Conclusion: The results clarified the positive effect of bio synthesized PsAgNPs on *M. incognita* juveniles. More research needs to determine the long run effect.

Key Words: *Meloidogyne incognita*; Silver nanoparticles; *Photobacterium luminescens*; Bionanometricides

INTRODUCTION

The development of diseases caused by multiple pathogens, including Alternaria blight (*Alternaria alternata*), collar rot (*Sclerotium rolfsii*), powdery mildew (*Erysiphe polygoni*), [1] and root-knot disease caused by *Meloidogyne incognita* [2]. Root-knot nematode *Meloidogyne incognita* represents one of the most significant genera of plant-parasitic nematodes on various crops, as it is widespread and poses a threat to thousands of plant species. *Meloidogyne* species are obligatory sedentary endoparasites that infect over 3000 plant species worldwide [3]. As a result of their infection of the root system, which absorbs water and nutrients, the entire plant is harmed. Due to the completion of two or more life cycles in a single growing season and high female fertility, their population increases rapidly. As a result, crop yield declines cause huge financial losses of billions of dollars all over the world [4].

The use of chemical nematicides to control the pathogen has been restricted due to adverse environmental and health effects [5,6]. These biologically disruptive forces pave the way for inexcusably poor well-being, stability, and an array of environmental issues [7]. The potential threat to nontarget organisms has prompted researchers to seek out novel ecofriendly or less toxic nematode control methods. To mitigate this issue, eco-friendly methods and sustainable crop protection technologies must be incorporated into the current agricultural system. These methods and technologies can be used to protect crops from nematode damage and maintain plant growth and yield. In the past few years, it's become clear that nanotechnology has the potential

to change the way farming is done [8].

Agriculture and disease management are the most significant applications of nanotechnology [9,10]. Agriculture systems have the potential to utilise nanoparticles with a small size and a large surface area of 1–100 nm. Multiple studies have found that the nonmaterial is an alternative to chemical pesticides, making it an excellent option for the development of new pesticides. Silver nanoparticles are recognised for their broad spectrum of antimicrobial and plant disease management properties [11,12]. Silver nanoparticles synthesised from plants are significantly less toxic than silver ions, whereas their antimicrobial properties are significantly enhanced [13,14]. In contrast to chemical pesticides, they can be used to control a variety of plant diseases in a sustainable manner due to their diverse modes of inhibition against phytopathogens [15]. To date, there have been very few investigations into the suitability of nanosilver for plant disease control [16]. Even though there are both chemical and physical ways to make silver nanoparticles, all of them use dangerous chemicals and require a lot of energy [17].

Sharon et al., [18] describe nanotechnology as a promising new technique in the field of plant pathology because it can provide controlled delivery of functional molecules or serve as a diagnostic tool for disease detection by producing novel materials. Numerous studied and employed nanoparticles in bio-systems exhibit potent inhibitory and antimicrobial properties effectiveness of colloidal nanoparticles against *Sphaerotheca pannosa* var. *rosae*-caused rose powdery mildew. Colloid nanoparticles are well dispersed and

Department of Post Graduate and Research Centre of Zoology, Jayaraj Annapackiam College for Women (Autonomous), Affiliated to Mother Teresa Women's University Kodaikanal, Periyakulam, Tamil Nadu, India

Correspondence: S. Iruthaya Kalai Selvam, Department of Post Graduate and Research Centre of Zoology, Jayaraj Annapackiam College for Women (Autonomous), Affiliated to Mother Teresa Women's University Kodaikanal, Periyakulam, 625601, Tamil Nadu, India, Email: iruthayakalaisevam@gmail.com; vinothinikerthan@gmail.com

Received: 02-Nov-2022, Manuscript No. AGBIR-22-80744; **Editor assigned:** 07-Nov-2022, Pre QC No. AGBIR-22-80744(PQ); **Reviewed:** 21-Nov-2022, QC No. AGBIR-22-80744; **Revised:** 28-Nov-2022, Manuscript No. AGBIR-22-80744 (R); **Published:** 05-Dec-2022, DOI:10.35248/0970-1907.23.38.395-400



This open-access article is distributed under the terms of the Creative Commons Attribution Non-Commercial License (CC BY-NC) (<http://creativecommons.org/licenses/by-nc/4.0/>), which permits reuse, distribution and reproduction of the article, provided that the original work is properly cited and the reuse is restricted to noncommercial purposes. For commercial reuse, contact reprints@pulsus.com

stable [19]. The adhesive properties of silver nanoparticles on bacteria and fungi are studied. Anderson [20] classifies nanoparticles as pesticides. Now widely accepted as a substitute for agrochemicals, silver eliminates unwanted microorganisms in planter soils and hydroponics systems. Silver nanoparticles are also an excellent stimulant of plant growth. Silver nanoparticles have potent antibacterial, antifungal, insecticidal, and nematocidal properties [21-27].

Because of their compact size and large area to volume, AgNPs can able to bind closely with the membranes of microorganisms, which results in antibacterial effects. Smaller particles with a greater surface area possess antibacterial properties. Antibacterial properties have been proven for NPs such as AgNPs and AuNPs against both gram-positive and gram-negative bacteria. In recent years, NPs' anticancer properties have been established [28,29]. The goal of this study is to make silver nanoparticles that work against the root-knot nematode, *Meloidogyne incognita*.

MATERIALS AND METHODS

H. indica was raised by *Galleria mellonella* larvae and incubated in a BOD incubator at 20°C. The initial stages of the symbiotic bacteria *P. luminescence* were isolated from a newly emerged Infective Juveniles (IJs) of *H. indica* that had been decontaminated by a 10% sodium hypochlorite solution for ten minutes and then rinsed 2-3 times with sterile water. Secondary stages were obtained from *H. indica*-based monogenic cultures. As per Akhurst [30], surface-sterilized IJs were made into a powder, and a loop of the subsequent liquid was smeared on NBTA (nutrient agar of 0.004 percent 2, 3, 5-triphenyltetrazolium chloride as well as 0.025% bromothymol blue) agar plates. Selecting and subculturing single colonies on new NBTA media was continuous until pure colonies of *P. luminescence* were attained. Finally, the culture was kept at 70°C using a glycerol stock.

Molecular characterization of *P. luminescence* ON929969

Using the DNeasy Blood and Tissue Kit (QIAGEN, Hilden, Germany) per the manufacturer's instructions, bacterial DNA was isolated from a 2-day-old culture. To amplify the 16S rRNA gene, the primers 10F: 5'-AGTTTGATCATGGCTCAG ATTG-3' (forward) and 1507R: 5'-TACCTTGTTACGACT TCACCCAG-3' (reverse) was used. PCR master mix contained 16.8 l of nuclease-free H₂O, 1 l of bovine serum albumin, 2.5 l of 10 dream Taq buffer, 0.5 l of 10 mM dNTPs, 0.75 l of each forward and reverse primer, 0.2 l of dream Taq DNA polymerase, and 2 l of DNA. Following a 3-minute cycle at 94 degrees Celsius, there were 33 cycles of 60 seconds at 94 degrees Celsius, 60 seconds at 55 degrees Celsius, and two minutes at 72 degrees Celsius, with a final 10-minute extension at 72 degrees Celsius. All PCR products were sequenced and submitted to Genbank with the accession number ON929969.

Synthesis and optimization of PsAgNPs

The initial components were composed of silver nitrate (AgNO₃). *P. luminescence* was grown for 48 hours at 28°C with stirring in an Erlenmeyer flask of 1 litre capacity that was poured with 500 ml of Broth culture. The capability of the isolated bacterial strain to reduce metal ions and aggregate nanoparticles was evaluated. On the basis of early tests, *P. luminescence* ON929969 was chosen as a potential strain for nanomaterial manufacturing. An Erlenmeyer flask containing LB broth was given a fresh inoculation of the strain, and the flask was then placed in an incubator at 37°C for a period of twenty-four hours. After incubation, the microbial culture filtrates were recovered by centrifuging by 6000 rpm for 10 mins. Then, supernatant mixtures for the production of PsAgNPs were produced by combining 90 ml of 1 Mm AgNO₃ and 10 ml of centrifuged bacteria free supernatant in a 250 ml Erlenmeyer flask, then incubating them at 30°C for 24 hours. Then, the bioreduction response was observed by detecting the reaction mixture's colour variation and UV-Vis absorbance. The absorbance intensity of the UV-Vis spectra was used to tune a number of reaction parameters, such as pH (5-9) and metal ion concentration (1 mM-5 mM), to get the best size distribution of NPs with the highest yield [31,32].

Instrumentation

Using a JASCO V-650 UV-Visible Spectrophotometer, the optical properties of synthesised NPs were examined at wavelengths ranging from 300 to 700 nm. Utilizing FT-IR spectroscopy, the surface chemistry and involvement of bacterial proteins in the reduction and stability of NPs were investigated. The wavelength spectrum of the cell-free supernatant prior to and after the

addition of metal ion solution AgNO₃ was recorded using Perkin Elmer manufacture model spectrum 22575927 RX1 (wavelength range of 4000 cm⁻¹ to 400 cm⁻¹). Using X-ray diffraction, the dimensions of biologically produced PsAgNPs with h, k, and l values were determined. The diffraction pattern was made in Cu under the following conditions: 40 kV, 30 mA, K-alpha radiation, and particle size (L), which was calculated using the Debye-equation Scherrer's and applied to an Ag nanoparticle.

$$D = k\lambda / \beta \cos \theta$$

λ -Is the x-ray wavelength

β -Is the Full Width at Half Maximum (FWHM) and

θ -Is the diffraction angle

A Scanning Electron Microscopy (SEM) investigation was performed with a JEOL JSM-6390 model. By depositing a small amount of sample on the copper grid, a thin carbon-coated film was created. Before analysis, the sample film on the SEM grid was dried for 5 minutes under a mercury lamp [33]. Blotting paper was used to get rid of any extra water.

Against *Meloidogyne incognita*: The root knot nematode

Maintenance of pure culture *M. incognita*: Tomato plants raised in greenhouses at a temperature of 28°C provided the inoculum needed to raise the pure culture of *M. incognita*. The roots of tomatoes with prominent galls were selected, washed thoroughly, and examined under a microscope for the presence of egg masses. Galls that revealed the projecting bodies of mature females covered with a gelatinous matrix were excised and a single egg mass were transplanted to embryo cups containing half the volume of water. For the purpose of maintaining a pure culture of root knot nematode, the juveniles hatched from the egg mass were collected and injected into four-week-old tomato (variety PKM1) seedlings. The containers were kept in a greenhouse environment and were constantly watered. The plants were plucked and rinsed clean of dirt 45 days following inoculation. The mature egg masses were extracted with care, put into Petri dishes containing a sufficient amount of distilled water, and incubated under laboratory conditions. The hatched eggs and juveniles were used in several experiments done for this study.

J2 mortality assay

The various concentrations of Bio PsAgNPs were collected individually in sterile Petri dishes (5 cm in diameter) containing 5 mL per Petri dish. The newly hatched second stage juveniles (J2) of *M. incognita* obtained through pure culturing of root knot nematode were transferred at a rate of 100 J2/ Petri dish to investigate the effect of AgNPs on the juveniles of *M. incognita* under laboratory conditions (28°C). To examine the larvicidal impact of bio PsAgNPs, each treatment was duplicated three times in CRD. Observations were made on the mortality of *M. incognita* juveniles every 24 hours, and the percentage mortality of juveniles was calculated after confirming the irreversible reaction of *M. incognita* upon exposure to the bio-synthesised PsAgNPs.

RESULTS

Molecular characterization and synthesis of PsAgNPs

After isolation and initial morphology verification, the isolated strain was proven to be *P. luminescence* ON929969 by molecular authentication. Further *P. luminescence* ON929969 was developed for the preparation of nanomaterials with the desired structure. The extracellular products of *P. luminescence* strain ON929969 were utilised for the sustainable synthesis of PsAgNPs. After the addition of extracellular components to the metal ions (1 mM AgNO₃), the reaction mixtures changed colour due to the activation of Surface Plasmon Resonance (SPR). After 24 hours of incubation, PsAgNPs exhibited a dark brownish hue.

UV-visible spectroscopy

Significantly, UV-visible spectroscopic investigation has revealed that PsAgNPs have a prominent SPR peak at 430 nm. At 37°C ± 2, the produced particles were extremely stable. In order to maintain reproducibility, the best conditions for synthesising AgNPs with a narrow size distribution in a shorter period were determined to be pH 9. For AgNPs, the metal ion concentration is 1 mM, and the incubation duration is 24 hours. The optimally synthesised

NPs generated a strong resonance centred at approximately 430 nm, the intensity of which grew with incubation time. The reported results for the culture extract of *P. luminescens* are very indicative of the importance of developing a rapid approach for PsAgNPs (Figure 1).

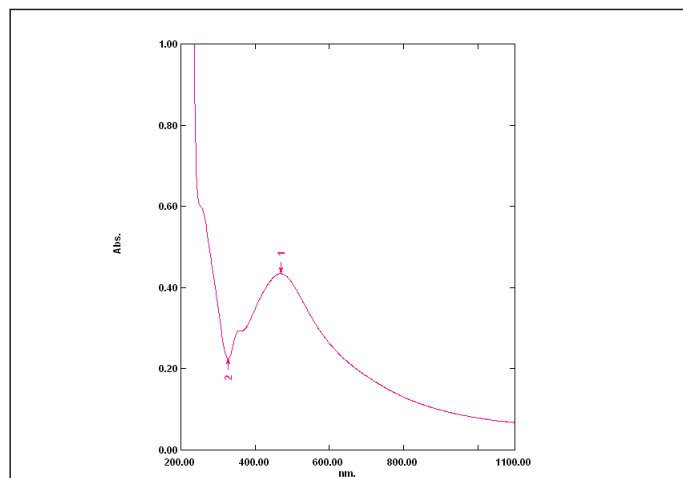


Figure 1) The UV-Vis spectrum of synthesized bio PsAgNPs recorded at room temperature

FTIR

The FTIR spectra of produced AgNPs showed the presence of frequency ranges at 3398.50, 2960.04, 1641.39, 1540.52, 1387.38, 1230.45, 1077.11, and 607.03 cm⁻¹. The band located at 3398.50 cm⁻¹ corresponds to the RCO-OH of carboxylic acids. The band at 2960.04 cm⁻¹ indicates RCH₂CH₃ group stretching in alkanes. The band at 1641.39 cm⁻¹ corresponds to the RCONHR'6 vibration of the group of amides. The band located at 1540.52 cm⁻¹ corresponds to the N-O stretching vibration of various groups. The frequency of 1387.38 cm⁻¹ corresponds to the S=O stretching vibration of various groups. The frequency at 1077.11 cm⁻¹ belongs to the RNH₂ vibration of the amines group. The band at 607.03 cm⁻¹ indicates the C-H stretching vibrations of the alkynes group. The presence of carboxylic acids, aromatics, alcohols, alkenes, alkynes and alkyl halides is also revealed by FTIR peaks (Figure 2).

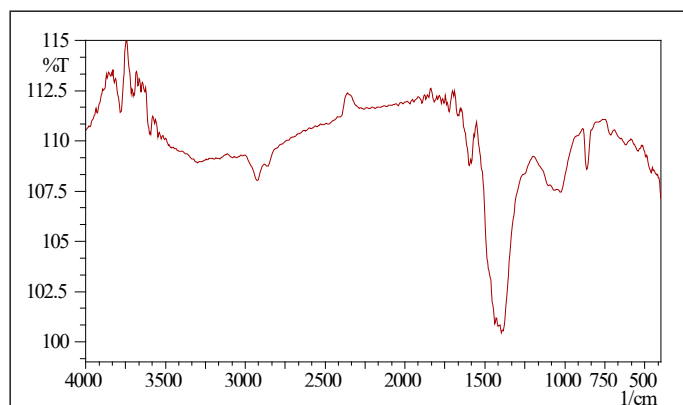


Figure 2) FTIR analysis of cell-free supernatant of synthesized NPs using *P. luminescence* ON929969

XRD

In the 2θ range of the XRD pattern, three Bragg's reflections were found at 38.1, 77.4, 46.4, and 64.5, corresponding to miller indices of (111), (311), (200), and (220). Consequently, this XRD pattern clearly demonstrates the formation of crystalline AgNPs, and it corresponds well with their typical JCPDS values. The width of XRD peaks is typically proportional to crystallite size. Using the half width of the diffraction peaks, the average crystallite diameter was calculated using the Debye-Scherrer equation:

$$D = (k\lambda) / (\beta \cos \theta) \text{ Eq-1}$$

Where, D is mean crystallite size of the powder;

λ is the wavelength of CuKα;

β is the full width at half-maximum;

θ is the Bragg diffraction angle; k is a constant.

The (111) plane was chosen for the crystal size calculation. The Debye-Scherrer equation reveals that the average crystallite size of produced AgNP is 22.38 nm (Figure 3).

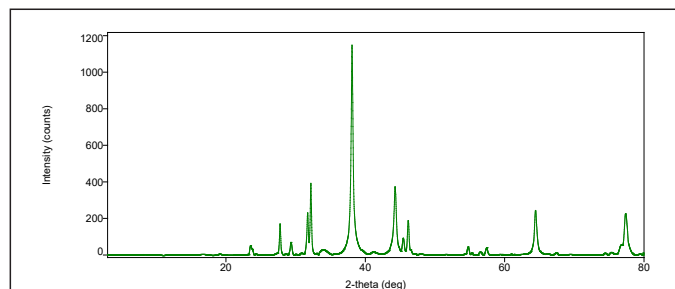


Figure 3) X-ray Diffraction analysis of synthesized bio PsAgNPs displays the equivalent diffraction value of face centered cubic crystalline structures

SEM analysis

The results clearly demonstrate that the majority of AgNPs were aggregated spherical nanoparticles with a distinct size distribution and an average diameter of approximately 15.5 nm. The surface shape of agglomerated nanoparticles has a significant influence on their biological uses (Figures 4a and 4b).

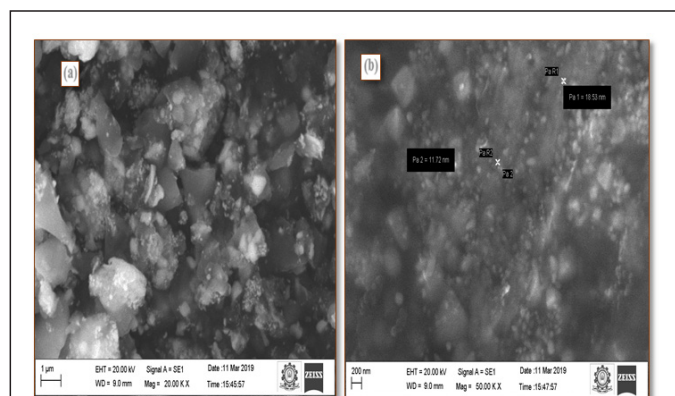


Figure 4) SEM micrographs displays well-distributed spherical AgNPs. Note: (a) size of the nanoparticles, (b) diameter of the nanoparticles

Antinematic characteristics

The larvicidal effect of root knot nematode *Meloidogyne incognita* was examined by the *P. luminescens*-mediated synthesis of AgNPs with favourable characteristics of AgNPs.

Influence on juveniles of *M. incognita*

All concentrations of AgNPs utilising *P. luminescens* caused mortality of *M. incognita* juveniles during all periods of exposure relative to the untreated control and varied considerably from one another. The effect of bio PsAgNPs had a direct correlation between the death rate of J2 of *M. incognita* and exposure concentrations/duration. In contrast to water screening, 0.1 g/ml of bio PsAgNP was ineffective even after 72 hours. Juvenile mortality began at 0.2 g/ml, increased with rising bio PsAgNP concentration and time (p 0.05), and reached 100% at concentrations of 2 g/ml and higher after 24 hours. There was 100 percent death of *M. incognita* juveniles at higher concentrations of 2 and 3 g/ml of bio-synthesized AgNPs during the shortest duration of time of 24 hours, and this tendency was maintained throughout the exposure period. Similarly, the lower concentrations of 0.1 and 0.2 g/ml also caused 100 percent mortality in *M. incognita* juveniles (Table 1 and

Figure 5). The relationship between time and bio PsAgNP concentration was statistically significant ($p < 0.05$).

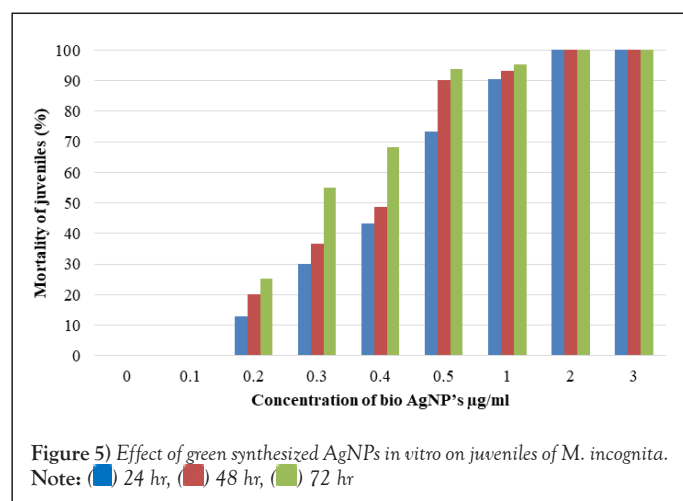


Table 1
Effect of bio synthesized PsAgNPs *in vitro* on juveniles of *M. incognita*

Concentration of bio AgNP's µg/ml	Mortality of juveniles (%) at different intervals (hours)		
	24 hr	48 hr	72 hr
0	0	0	0
0.1	0	0	0
0.2	13.00	20.23	25.35
0.3	30.00	36.70	55.00
0.4	43.30	48.72	68.30
0.5	73.2	90.30	93.70
1.0	90.42	93.15	95.43
2.0	100	100	100
3.0	100	100	100

Note: Control (no AgNP, water alone); Means are the three-replication averages; The data was subjected to 9×3 (bio PsAgNP concentration \times incubation time).

DISCUSSION

The nanoparticles synthesised by the *P. luminescens* strain KPR-8B were identified by their colour changes from pale yellow to purple for AuNPs and brownish for AgNPs after 24 hours [32]. 24 hours after being incubated, *X. stockiae* AgNPs had a dark brownish color, but XsAuNPs had a pinkish colour [31].

Earlier studies using *P. aeruginosa* have demonstrated the production of AgNPs with a prominent and broad peak between 430 nm and 450 nm after 72 hours of incubation [34]. In the current investigation, after 24 hours of incubation, the same peak for PsAgNPs was seen at 430 nm. The SPR peak for *P. luminescens* KPR-8B generated AuNPs and AgNPs was 560 and 440 nm after 24 h of incubation.

The FTIR spectra of produced NPs exhibited variations in the stretches, which are mostly the result of the interaction between metal ions and bacterial proteins [35]. FTIR analysis revealed that amines, alkynes, and alkyl halides mostly contribute to the production of AuNPs and AgNPs by the *P. luminescens* KPR-8B strain. In the infrared area of the electromagnetic spectrum, the amide bonds between amino acid residues in proteins provide well-known signals. The bands correspond to the relative stretching vibrations of primary and secondary amines [31]. We compared the FTIR spectra of bacterial supernatant and AgNPs and found that the main peaks were between 1540 cm^{-1} and 573 cm^{-1} . This shows that the main functional groups that make up the nanoparticles are located between these two points. The XRD patterns shown here are consistent with previous findings [36]. The results of XRD and SPR showed that the size range of nanoparticles is limited [37].

The nanoparticle diameters in the HRTEM micrographs ranged from 14 to

46 nm for AuNPs and 17 to 40 nm for AgNPs. Similarly, *Klebsiella pneumoniae* produced AgNPs ranging in size from 28.2 to 122 nm, with an average size of 52.5 nm [38]. In addition to a reduced metal ion concentration, El-Shanshoury et al. [39] found that *R. capsulata*-derived AuNPs had a spherical morphology and a size range of 10–20 nm.

The findings of Ardakani [40] and Cromwell et al., [27], which evaluated the antimicrobial capabilities of metal AgNPs against *M. incognita* and *M. graminicola*, support the current findings. Yeon et al., [41] and Lim et al., [42] both suggested that AgNPs could be the metal nanoparticles that cause oxidative stress in phytonematode cells and have a direct effect on how nematodes use energy. Widespread use of chemical pesticides and herbicides on farmland to eliminate weeds and pests and maximize potential output. Over exploitation, on the other hand, was harming soil health. A nano-pesticide is an agrochemical combination that is used to solve problems caused by traditional pesticides [43]. Recently, several nanometer-sized materials, such as surfactants, organic polymers, and minerals, have been used in the formulation of nano-pesticides [44]. The new generation of nanopesticides are field and target specific in action against insects, and they do not harm other agriculturally important insects in the soil [45,46]. Malaria, dengue, and filariasis are caused mostly by *Aedes aegypti*, *Aedes stephensi* and *Culex quinquefasciatus*, respectively, in urban areas. Every year, these diseases cause economic damage in India [47]. The current ecofriendly symbiotic bacterium, KPR-8B derived materials, was tested against vectors, *Aedes*, *Anopheles* and *Culex* species.

In this manner, the current *P. luminescens* was tested for its larvicidal potential against three different vectors. The larvicidal effect of KPR-8B synthesised AuNPs and AgNPs on the 4th instar larvae of *Aedes aegypti*, *Aedes stephensi* and *C. quinquefasciatus* was investigated. In general, 4th instar larvae are thought to be more immune-competent than younger larvae [48]. The larvicidal bioassays revealed that KPR-8B derived AgNPs had the greatest larvicidal effect against *Aedes aegypti*, with LC50 values of (lg/ml): 7.213 and LC90 values of (lg/ml): 31.232. Against *Aedes aegypti*, the reported inhibitory concentrations (lg/ml) of KPR-8B derived AuNPs produced substantial fatal values (lg/ml) LC50; 5.041 and LC90; 28.657. The entomopathogenic bacterium suspensions of *P. luminescens* TTO DSM15139 [49] and *Xenorhabdus nematophilus* ATCC 19061 [50] were highly toxic to *Aedes aegypti* 3rd instar larvae.

In addition, Vani and Lalithambika [51] found that protein isolated from *Xenorhabdus* strains caused the greatest mortality (93.32%) in 3rd instar *A. gambiae* larvae. Previous research found that protein toxins isolated from *X. nematophilus* strain A24 were highly toxic when injected into *G. mellonella* and *Helicoverpa armigera* [52,53]. Yooyangket et al., [54] reported similar findings when testing the toxicity of *Xenorhabdus* and *Photorhabdus* isolates against *Aedes aegypti* and *Aedes albopictus* larvae. After 96 hours of exposure to *X. stockiae* and *P. luminescens*, they discovered the highest larval mortality of *Aedes aegypti* (99%) and *Aedes albopictus* (98%). Consequently, the current larvicidal capability of the symbiotic bacteria *P. luminescens* functions as a biocontrol agent *via* their active extracellular proteins or enzymes. Nanoparticles have numerous applications in medicine, drug delivery and most importantly, as a pesticide against a variety of pests [55].

The methylene chloride extract of *C. sinuosa* was more active than that of *C. mediterranea*, and hexane: methylene chloride: ethyl acetate (1:0.5:0.5, v/v/v) was the most efficient eluent. The third portion of this eluent killed 87.5% of *M. incognita* after 12 h and 100% after 24 and 72 h. This fraction contained seven bioactive components. *C. sinuosa*'s silver nanoparticles could be employed as nematicides [56]. The highest concentration (90%) of silver nanoparticles, Poly Vinyl Pyrrolidone (PVP), fenamiphos and oxamyl resulted in 95, 87, 98 and 100% juvenile mortality after 72 h, while control mortality was 1.5%. In the experiment, fenamiphos, oxamyl and PVP paralysed juveniles that were not properly formed, and silver nanoparticles broke down the cell walls [57].

CONCLUSION

To conclude, during the present study, the culture extract of *P. luminescens* ON929969 are very indicative of the importance of developing a rapid approach for PsAgNPs. The results clarified the positive effect of bio synthesized PsAgNPs on *M. incognita* juveniles. Ultimately, AgNP may provide alternative to currently used chemical nematicides and resolve nematode problems on other crops. The presently utilized sources are cost

effective, biocompatible, eco-friendly and are useful for an alternative type of eco-friendly insect pest management programme. More research needs to determine the long run effect.

ACKNOWLEDGEMENTS

Sr. S. Iruthaya Kalai Selvam and A. Vinothini, extent their sincere thanks to the management, Jayaraj Annappackiam College for Women (Autonomous), Periyakulam, India for providing research facilities under BSR and DST-FIST support equipment's and the financial support under JACFRP.

FUNDING

Sr. S. Iruthaya Kalai Selvam and A. Vinothini, extent their sincere thanks to the management, Jayaraj Annappackiam College for Women (Autonomous), Periyakulam, India for providing research facilities under BSR and DST-FIST support equipment's and the financial support under JACFRP.

AUTHOR'S CONTRIBUTION

V and IKS planned, conceived and designed the manuscript. V carried out analysis, writing the manuscript, referencing setting, and editing of the manuscript. IKS helped in revision. All authors read, revised, and approved the final manuscript.

REFERENCES

- Khare MN, Tiwari SP, Sharma YK, et al. Disease problems in cultivation of celery (*Apium graveolens* L.) ajwain (*Trachyspermum ammi* L.), dill (*Anethum graveolens* L.), nigella (*Nigella sativa* L.), anise (*Pimpinella anisum* L.) and their management. *Int J Seed Spices*. 2015;5:34-36.
- Danish M, Alraf M, Robab MI, et al. Green synthesized silver nanoparticles mitigate biotic stress induced by *Meloidogyne incognita* in *Trachyspermum ammi* (L.) by improving growth, biochemical, and antioxidant enzyme activities. *ACS omega*. 2021;6(17):11389-11403.
- Dubreuil G, Deleury E, Magliano M, et al. Peroxiredoxins from the plant parasitic root-knot nematode, *Meloidogyne incognita*, are required for successful development within the host. *Int J Parasitol*. 2011;41(3-4):385-396.
- Abad P, Gouzy J, Aury JM, et al. Genome sequence of the metazoan plant-parasitic nematode *Meloidogyne incognita*. *Nat Biotechnol*. 2008;26(8):909-915.
- Ebone LA, Kovaleski M, Deuner CC. Nematicides: history, mode, and mechanism action. *PST*. 2019;6(2):91-97.
- Stirling GR. Biological control of plant-parasitic nematodes. In *Diseases of nematodes 2018*. CRC Press. 103-150.
- Manczinger L, Antal Z, Kredics L. Ecophysiology and breeding of mycoparasitic *Trichoderma* strains. *Acta Microbiol Immunol Hung*. 2002;49(1):1-14.
- Norman S, Hongda C. IB in depth special section on nanobiotechnology. *Ind Biotechnol*. 2013;9:17-18.
- Nair R, Varghese SH, Nair BG, et al. Nanoparticulate material delivery to plants. *Plant Sci*. 2010;179(3):154-163.
- Ghormade V, Deshpande MV, Paknikar KM. Perspectives for nanobiotechnology enabled protection and nutrition of plants. *Biotechnol Adv*. 2011;29(6):792-803.
- Navrotsky A. Nanomaterials in the environment, agriculture, and technology (NEAT). *J Nanoparticle Res*. 2000;2(3):321-333.
- Choi M, Shin KH, Jang J. Plasmonic photocatalytic system using silver chloride/silver nanostructures under visible light. *J Colloid Interface Sci*. 2010;341(1):83-87.
- Jain S, Mehata MS. Medicinal plant leaf extract and pure flavonoid mediated green synthesis of silver nanoparticles and their enhanced antibacterial property. *Sci Rep*. 2017;7(1):1-3.
- Singh H, Du J, Singh P, et al. Ecofriendly synthesis of silver and gold nanoparticles by *Euphrasia officinalis* leaf extract and its biomedical applications. *Artif Cells Nanomed Biotechnol*. 2018;46(6):1163-1170.
- Park HJ, Kim SH, Kim HJ, et al. A new composition of nanosized silica-silver for control of various plant diseases. *Plant Pathol J* 2006;22(3):295-302.
- Lamsal K, Kim SW, Jung JH, et al. Application of silver nanoparticles for the control of *Colletotrichum* species *in vitro* and pepper anthracnose disease in field. *Mycobiology*. 2011;39(3):194-199.
- Ahmed S, Ahmad M, Swami BL, et al. A review on plants extract mediated synthesis of silver nanoparticles for antimicrobial applications: a green expertise. *J Adv Res*. 2016;7(1):17-28.
- Sharon M, Choudhary AK, Kumar R. Nanotechnology in agricultural diseases and food safety. *J Phytol*. 2010;2(4).
- Kim SH, Choi MC, Yoo JS, et al. Apparatus and method for improving fourier transform ion cyclotron resonance mass spectrometer signal. US patent. 2010.
- Anderson CB. Regulating nano-silver as a pesticide. EDF.2009.
- Kim SH, Lee HS, Ryu DS, et al. Antibacterial activity of silver-nanoparticles against *Staphylococcus aureus* and *Escherichia coli*. *Microbiol Biotechnol Lett*. 2011;39(1):77-85.
- Sharma D, Ledwani L, Bhatnagar N. Antimicrobial and cytotoxic potential of silver nanoparticles synthesized using *Rheum emodi* roots extract. *Front Chem*. 2015;24(2):121.
- Sayed SR, Bahkali AH, Bakri MM, et al. Antibacterial activity of biogenic silver nanoparticles produced by *Aspergillus terreus*. *Int J Pharmacol*. 2015;11(7):858-863.
- Pulit J, Banach M, Szczygłowska R, et al. Nanosilver against fungi. Silver nanoparticles as an effective biocidal factor. *Acta Biochim Pol*. 2013;60(4).
- Balashanmugam P, Balakumaran MD, Murugan R, et al. Phytochemical synthesis of silver nanoparticles, optimization and evaluation of *in vitro* antifungal activity against human and plant pathogens. *Microbiol Res*. 2016;192:52-64.
- Borase HP, Patil CD, Salunkhe RB, et al. Mosquito larvicidal and silver nanoparticles synthesis potential of plant latex. *J. Entomol. Acarol. Res*. 2014;46(2):59-65.
- Cromwell WA, Yang J, Starr JL, et al. Nematicidal effects of silver nanoparticles on root-knot nematode in bermudagrass. *J Nematol*. 2014;46(3):261.
- Kim JS, Kuk E, Yu KN, et al. Antimicrobial effects of silver nanoparticles. *Nanomed-Nanotechnol*. 2007;3(1):95-101.
- Kuo WS, Chang CN, Chang YT, et al. Antimicrobial gold nanorods with dual-modality photodynamic inactivation and hyperthermia. *Chem comm*. 2009(32):4853-4855.
- Akhurst RJ. Morphological and functional dimorphism in *Xenorhabdus* spp., bacteria symbiotically associated with the insect pathogenic nematodes *Neoplectana* and *Heterorhabditis*. *Microbiology*. 1980;121(2):303-309.
- Chandrakasan G, Seetharaman P, Gnanasekar S, et al. *Xenorhabdus stockiae* KT835471-mediated feasible biosynthesis of metal nanoparticles for their antibacterial and cytotoxic activities. *Artif Cells Nanomed Biotechnol*. 2017;45(8):1675-1684.
- Aiswarya D, Raja RK, Kamaraj C, et al. Biosynthesis of gold and silver nanoparticles from the symbiotic bacterium, *Photorhabdus luminescens* of Entomopathogenic Nematode: Larvicidal Properties against three mosquitoes and *Galleria mellonella* Larvae. *J Clust Sci*. 2019;30(4):1051-1063.
- Padalia H, Moteriya P, Chanda S. Green synthesis of silver nanoparticles from marigold flower and its synergistic antimicrobial potential. *Arab J Chem*. 2015;8(5):732-741.
- Husseiny MI, Abd El-Aziz M, Badr Y, et al. Biosynthesis of gold nanoparticles using *Pseudomonas aeruginosa*. *Spectrochim Acta A Mol Biomol Spectrosc*. 2007;67(3-4):1003-1006.
- Vignesh V, Sathiyarayanan G, Sathishkumar G, et al. Formulation of iron oxide nanoparticles using exopolysaccharide: evaluation of their antibacterial and anticancer activities. *RSC Advances*. 2015;5(35):27794-27804.
- Shankar SS, Ahmad A, Sastry M. Geranium leaf assisted biosynthesis of silver nanoparticles. *Biotechnol Prog*. 2003;19(6):1627-1631.
- Philip D, Unni C. Extracellular biosynthesis of gold and silver nanoparticles using *Krishna tulsi* (*Ocimum sanctum*) leaf. *Physica E: Low-dimensional Systems and Nanostructures*. 2011;43(7):1318-1322.

38. Murdock RC, Braydich-Stolle L, Schrand AM, et al. Characterization of nanomaterial dispersion in solution prior to *in vitro* exposure using dynamic light scattering technique. *Toxicol Sci.* 2008;101(2):239-253.
39. Shanshoury RE, Elsilk SE, Ebeid ME. Extracellular biosynthesis of silver nanoparticle using *Escherichia coli* ATCC, 8739, *Bacillus subtilis* ATCC, 6633, and *Streptococcus thermophilus* ESh1 and their antimicrobial activity. *ISRN Nanotechnology.* 2011;2011:7.
40. Ardakani AS. Toxicity of silver, titanium and silicon nanoparticles on the root-knot nematode, *Meloidogyne incognita*, and growth parameters of tomato. *Nematology.* 2013;15(6):671-677.
41. Roh JY, Sim SJ, Yi J, et al. Ecotoxicity of silver nanoparticles on the soil nematode *Caenorhabditis elegans* using functional ecotoxicogenomics. *Environ Sci Technol.* 2009;43(10):3933-3940.
42. Lim D, Roh JY, Eom HJ, et al. Oxidative stress-related PMK-1 P38 MAPK activation as a mechanism for toxicity of silver nanoparticles to reproduction in the nematode *Caenorhabditis elegans*. *Environ Toxicol Chem.* 2012;31(3):585-592.
43. Ishaaya I, Nauen R, Horowitz AR. Insecticides design using advanced technologies. *Springer Sci Rev;* 2007.
44. El-Sadawy HA, El Namaky AH, Hafez EE, et al. Silver nanoparticles enhance the larvicidal toxicity of *Photorhabdus* and *Xenorhabdus* bacterial toxins: an approach to control the filarial vector, *Culex pipiens*. *Trop Biomed.* 2018;35(2):392-407.
45. Kah M, Beulke S, Tiede K, et al. Nanopesticides: state of knowledge, environmental fate, and exposure modeling. *Crit Rev Environ Sci Technol.* 2013.
46. Tripathi M, Kumar S, Kumar A, et al. Agro-nanotechnology: a future technology for sustainable agriculture. *Int J Curr Microbiol Appl Sci.* 2018;7:196-200.
47. Govindarajan M, Rajeswary M, Muthukumaran U, et al. Single-step biosynthesis and characterization of silver nanoparticles using *Zornia diphylla* leaves: A potent eco-friendly tool against malaria and arbovirus vectors. *J Photochem Photobiol Biol.* 2016;161:482-489.
48. Deepak P, Sowmiya R, Balasubramani G, et al. Mosquito-larvicidal efficacy of gold nanoparticles synthesized from the seaweed, *Turbinaria ornata* (Turner) J Agardh 1848. *Part Sci Technol.* 2018;36(8):974-980.
49. Fischer-Le Saux M, Viallard V, Brunel B, et al. Polyphasic classification of the genus *Photorhabdus* and proposal of new taxa: *P. luminescens* subsp. *luminescens* subsp. nov., *P. luminescens* subsp. *akhurstii* subsp. nov., *P. luminescens* subsp. *laumondii* subsp. nov., *P. temperata* sp. nov., *P. temperata* subsp. *temperata* subsp. nov. and *P. asymbiotica* sp. nov. *Int J Syst Evol Microbiol.* 1999;49(4):1645-1656.
50. Thomas GM, POINAR JR GO. *Xenorhabdus* gen. nov., a genus of entomopathogenic, nematophilic bacteria of the family Enterobacteriaceae. *Int J Syst Evol Microbiol.* 1979;29(4):352-360.
51. Vani C, Lalithambika B. Effect of outer membrane vesicle proteins of *Xenorhabdus* bacteria against malarial vectors. *Int J Pharm Bio Sci.* 2014;5(4):1072-1080.
52. Khandelwal P, Banerjee-Bhatnagar N. Insecticidal activity associated with the outer membrane vesicles of *Xenorhabdus nematophilus*. *Appl Environ Microbiol.* 2003;69(4):2032-2037.
53. Hawlena H, Bashey F, Lively CM. The evolution of spite: Population structure and bacteriocin-mediated antagonism in two natural populations of *Xenorhabdus* bacteria. *Int J Org Evol.* 2010;64(11):3198-3204.
54. Yooyangket T, Muangpat P, Polseela R, et al. Identification of entomopathogenic nematodes and symbiotic bacteria from Nam Nao National Park in Thailand and larvicidal activity of symbiotic bacteria against *Aedes aegypti* and *Aedes albopictus*. *Plos one.* 2018;13(4):e0195681.
55. Singh HB, Mishra S, Fraceto LF, et al. Emerging trends in agri-nanotechnology: fundamental and applied aspects.
56. Ghareeb RY, Shams El-Din NG, Maghraby DM, et al. Nematicidal activity of seaweed-synthesized silver nanoparticles and extracts against *Meloidogyne incognita* on tomato plants. *Sci Rep.* 2022;12(1):1-6.
57. Hassan ME, Zawam HS, El-Nahas SE, et al. Comparison study between silver nanoparticles and two nematicides against *Meloidogyne incognita* on tomato seedlings. *Plant Pathol J.* 2016;15(4):144-151.